ISTS 2002-b-13

A Thrust Stand for Liquid Propellant Pulsed Plasma Thrusters

Hiroyuki Koizumi[*1], Akira Kakami, Kimiya Komurasaki[*2], and Yoshihiro Arakawa[*3]
University of Tokyo
7-3-1, Hongo, Bunkyo-ku, Tokyo 113-8656, JAPAN
(E-mail : koizumi@al.t.u-tokyo.ac.jp)

Abstract

A torsional-type thrust stand is designed, to precisely measure impulse bits produced by pulsed plasma thrusters (PPTs) in vacuum. This stand is capable of measuring low impulse ranging from 10 to 1000 μNs. Investigations into extremely low impulse measurement have been hampered by facility vibrations. We discuss about relation between background noise and vibrations induced by it, and optimum damping ratio, that makes Signal-to-Noise ratio maximum, is shown. Using this thrust stand, the performance of a liquid propellant PPT was measured.

1. Introduction

In recent years, researchers have become increasingly interested in Microthrusters. The motivations behind this initiative are the reduction of satellites' mass and size, including the propulsion devices, in order to accomplish far less expensive launch costs. In addition, modern missions require extremely precise thrust levels for attitude control and drag compensation.

In general, it is important to precisely measure thrusts for validation of thruster performance. However, it is difficult to accurately measure thrusts from microthrusters, which range from 10 to 1000 μNs. An early study of low thrust measurement was performed by Goddard Space Flight Center during the early 1970s [1]. To accurately measure thrusts, they used a thrust stand, which measured the reaction force exerted on the thruster. Recently, as microthrusters has got a great deal of attention, several studies of low thrust measurement using a thrust stand have been carried out [2]-[5]. However those devices were complex and expensive, and there has been no crucial method to measure low thrust level. On the other hand, in Japan, most of low thrust measurement has been performed by using a target pendulum [6][7]; it is installed downstream of the thruster, and momentum flux of the plume is measured. Although this method may be the simplest way to measure a thrust, it contains several problems; for instance a pressure rise between a thruster and the target, momentum accommodation of rebounding particles, and change of the flow field in the exhaust plume.

In this paper, we designed a thrust stand to accurately measure impulse bits produced by microthrusters, and measured impulse bits of 20 μNs level. To accomplish both accurate measurement and engineering simplicity, a passive damper was used in this study. A damper is a critical device for reducing undesirable vibrations. However there has been no study of quantitatively evaluating appropriate damping ratio of a thrust stand; several studies have taken little attention of its strength [3][4], or others have used complicate damping circuit [1][2][5]. Therefore we discuss the relation between background noise and induced vibration on the thrust stand. Finally optimum damping ratio, that makes Signal-to-Noise ratio maximum, is shown.

2. Principle of impulse measurement

A thrust stand based on a torsion balance measures a reaction force exerted on a thruster. A thruster is installed on the thrust stand, and impulse bit is calculated from the response by the reaction force of a thrust. Mechanism of the thrust stand and nomenclatures are shown in Fig. 1. A momentum equation of the balance is

$$J\ddot{\theta} + c\dot{\theta} + k\theta = T(t) \tag{1}$$

where θ is the angular deflection, J is moment of inertia, c is equivalent viscous damping, k is torsional spring rate, and $T(t)$ is time dependence torque exerted on the rotational axis. Since we measure the displacement of the balance, the preceding equation is multiplied by

*1 Graduate student, *2 Associate professor,
*3 Professor

distance l_m away from the rotational axis to the measurement point:

$$\ddot{x} + 2\varsigma\omega_0 \dot{x} + \omega_0^2 x = l_m T(t) / J \quad (2)$$

$$\omega_0 = \sqrt{\frac{k}{J}} \quad (3)$$

$$\varsigma = \frac{c}{2J\omega_0} \quad (4)$$

where x is displacement of the balance, ω_0 is natural angular frequency, and ζ is damping ratio. When, at $t = 0$, an impulse I is applied on a point, away from the rotational axis l_I, of the initially dormant balance, the solution is

$$x(t) = \frac{A}{\sqrt{1-\varsigma^2}} e^{-\varsigma\omega_0 t} \sin(\omega_0 \sqrt{1-\varsigma^2}\, t) \quad (5)$$

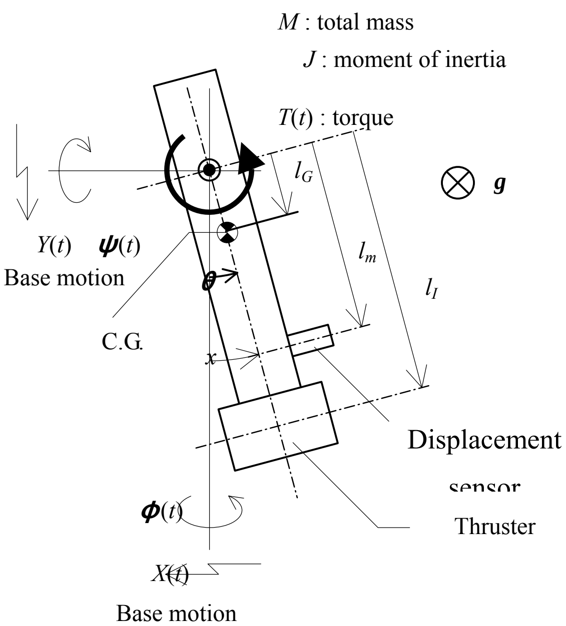

Fig. 1 Mechanics of a thrust stand

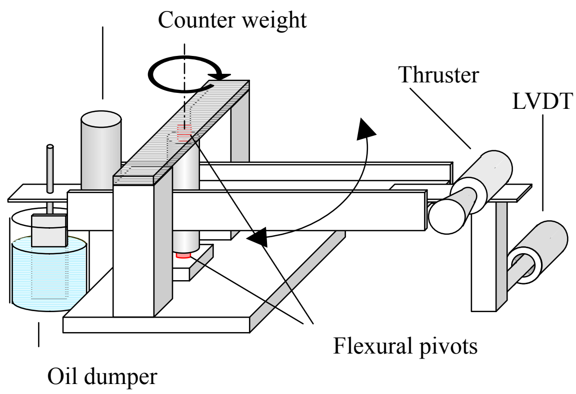

Fig. 2 Schematic of a thrust stand

$$A = \frac{I l_I l_m}{J\omega_0} \quad (6)$$

where A is the amplitude of the waveform when there is no damping. Therefore calculating the impulse bit requires measurement of ω_0, ξ, J, l_I, l_m, and A. However, only the amplitude is necessary, if the calibration is delivered at the same position as the force produced by the thruster, and ratio of the amplitude to the impulse is obtained.

3. Thrust Stand

The thrust stand dealt here can be separated into five systems.

A) Balance
B) Displacement sensor
C) Damper
D) Counterweight
E) Calibration equipment

A schematic diagram of the thrust stand is shown in Fig. 2. The explanation about each system is as follows.

A) The balance is a torsional balance, which vertically swings by a torsional restoring force. The rotational axis consists of two commercially available flexural pivots. Flexural pivots are made of flat crossed springs supporting sleeves, and there is no contact friction. Therefore they basically have no static friction and dynamic friction and each pivot has the torsional spring rate of 0.19 Nm/rad. The period of the balance was 3.0 s with the thruster and counterweight.

The balance consists of a torsional arm with H-beam section, on which a thruster is installed, and a rotational support tube, whose each end was connected to a supporting frame through the flexural pivots. Each part is made of aluminum: A5052.

B) Deflections of the balance were detected by a LVDT (linear variable differential transducer). Its linear operation range was 5 mm with the resolution from 0.1 to 0.3 μm. The transformer coils were attached to the stationary structure and the iron core was attached to the torsional arm. Calibration of the displacement was performed by using traverse equipment. However, this calibration is not necessary for the impulse measurement, because the impulse can be calculated from the voltage output of the LVDT.

C) An oil-filled fluidic damper was installed to dissipate undesirable vibrations induced by background vibrations. Its damping oil is a vacuum oil with vapor pressure of 1.3×10^{-8} Torr (25 $°C$).

D) Counterweights enable the rotating structure to be statically balanced, and reduce the influence of the background vibrational noise. When the base that supports a thrust stand has translational motion and inclination as shown in Fig. 1, torque exerted on the balance is

$$T(t) = l_G M\left(\ddot{X} + \theta \ddot{Y} + g(\phi + \theta\psi)\right) \qquad (7)$$

where l_G is the distance from the rotational axis to the center of gravity, M is the total mass of the balance, X and Y are motion of the base, ϕ and ψ are inclination angle of the base, and g is the gravitational constant. Therefore having the center of gravity on the rotational axis ($l_G \approx 0$) reduces the influence of the external vibrations.

E) Calibration was carried out by striking the thrust stand with an impact pendulum. The impact pendulum consists of a horizontal aluminum rod of 260 mg, which is suspended at each end by a nylon thread 0.45 m in length. The mass of the pendulum was determined by a precision analytic balance.

The impulse from the pendulum was determined from the deflection angle of the thread. The accuracy of this method was verified by other two methods. First, the instantaneous speed before and after the impact was monitored by a high speed CCD camera. Secondly, the impact pendulum impacted a force transducer. Time history of the force during the impact was recorded, and its integration was calculated as the impulse. The difference of the three methods was within 5.0% in the standard deviation. Especially the difference between the later two methods was within 2.0%.

4. Experimental method and Result

Impulse bits from a liquid propellant PPT was measured by using the thrust stand (A liquid propellant PPT is a kind of PPT using liquid propellant instead of solid propellant in order to supply the proper amount of propellant [8]). The thruster was installed on the balance beam 32 cm away from the rotational axis.

In early stage, experiments were performed without a damper and counterweights. There vibrational noise of the balance was higher than the impulse response from the thruster, and we could not measure the impulse bits. Thus we installed a damper and counterweights to reduce the vibrational noise. It is shown in Figure 3 that those had an effect to reduce the noise. Fig. 3 shows outputs of the LVDT during 150 s without PPT firing, vibrational noise. Four waveforms in Fig. 3 corresponds the four states of the thrust stand: a) without the damper and counterweight, b) with only the damper, c) with only the counterweights, and e) with both the damper and counterweights. Finally the vibrational noise was suppressed within 0.5 μm in standard deviation.

Figure 4 shows a typical thrust stand response to a PPT single shot with an impulse bit 27.8 μNs. Figure 5 shows the result of the measurement of impulse bits with the energy of 2.0, 3.1, and 4.5 J. The plots are the average of more than 15 shots with the error bars calculated from the standard deviation. Those standard deviations were 1.9, 1.5, and 1.5 μNs, correspond to the energy of 2.0, 3.1,

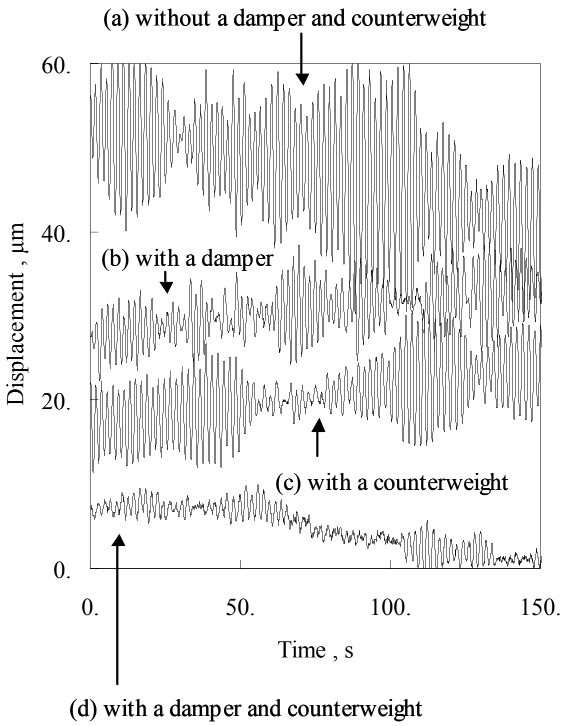

Fig. 3 induced vibrations on the thrust stand

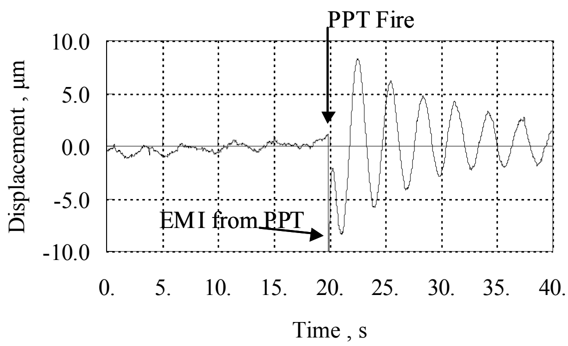

Fig. 4 The thrust stand response to a single PPT shot

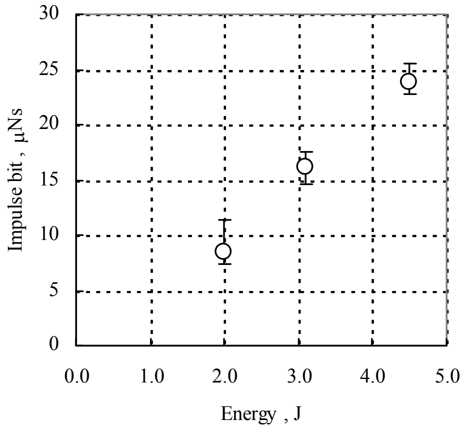

Fig. 5 The thrust stand measurement of liquid propellant PPT

and 4.5 J respectively. More than half of those deviations stemmed from the background vibrational noise, because standard deviation of the facility induced vibrations was approximately 0.5 μm, and it corresponded to 1.4 μNs.

In this study, averaged ratio of an impulse bit to the associated amplitude of the damping-vibration waveform was 2.8 μNs/μm. Since the operation range of the LVDT was ±2.5 mm, this thrust stand was enabled to measure impulse bits measurements up to 5000 μNs.

5. Discussion

5.1 Relation between damping ratio and facility induced vibrations on a thrust stand

One of the most important things to measure extremely low impulse is to raise SNR (Signal to Noise Ratio): that is to make vibrational-noise less than the response to the impulse. That vibrational noise is mainly induced by external vibrations, and here we call it induced vibration. In our study, counterweights and a damper were used in order to reduce that noise. Counterweights have the effect to reduce the noise by having the center of gravity zero. A damper has the effect to damp undesirable vibrations. However, the effect of a damper also works on the response to an impulse of PPT, and too strong damping effects adversely. Hence there must be an optimum damping strength, namely an optimum damping ratio: ζ_{opt}. However, there have been no studies to quantitatively evaluate that optimum value. Here we discuss about relation between damping ratio and facility induced vibrations on a thrust stand, and obtain the optimum damping ratio.

Here we evaluate the value of a signal and noise by using the dynamic properties of a thrust stand. First, we define a signal as the maximum value of the damped vibration of the balance:

$$x_{\max} = A\exp\left(-\varsigma\frac{Cos^{-1}(\varsigma)}{\sqrt{1-\varsigma^2}}\right) \tag{8}$$

Secondly, about the noise, we separate it two parts, that is 1) vibrational noise to which external vibrations delivered through the thrust stand and 2) noise with no relation to characteristics of the thrust stand, for instance electrical noise and the resolution of displacement sensor. About 1) we assume that the motion of the base is random and ergodic process, and it is transmitted through a stable linear system, namely the thrust stand; they are measured as a deflection of the balance. When we deal such a system subjected to random vibrations, it is useful to introduce a spectral density [9]. Here we define a spectral density of the base motion (inside of the parentheses of Eq. (7)) as $S(\omega)$. Thus a spectral density of the balance motion $S_x(\omega)$ can be calculated

$$S_x(\omega) = |H(\omega)|^2\left(l_G M\frac{l_m}{J}\right)^2 S(\omega) \tag{9}$$

where $H(\omega)$ is a frequency response function of the thrust stand:

$$H(\omega) = \frac{1}{\omega_0{}^2 + i2\varsigma\omega_0\omega - \omega^2} \tag{10}$$

Furthermore, between a spectral density and the associated mean square value, there is a relation [9]:

$$E(x^2) = \int_{-\infty}^{\infty} S_x(\omega)d\omega \tag{11}$$

where $E(x^2)$ is mean square value of the x. As a result, we obtain a mean square value of the induced vibration on the thrust.

$$\begin{aligned} E(x_n{}^2) &= \left(l_G M\frac{l_m}{J}\right)\int_{-\infty}^{\infty}|H(\omega)|^2 S(\omega)d\omega \\ &= N_m{}^2\frac{1}{\varsigma} \end{aligned} \tag{12}$$

$$N_m{}^2 = \left(l_G M\frac{l_m}{J}\right)\frac{\pi S_0}{2\omega_0{}^3} \tag{13}$$

where the integral inside of the upper equation was performed under the postulate that $S(\omega)$ is constant: S_0 [9]. N_m is standard deviation of vibration induced by the external noise at $\zeta = 1$. Hence it is an index expressing the amount of the external vibration. On the other hand, about 2), we assume it is constant: N_r, which is independent on damping ratio of a thrust stand. Since this noise includes electrical noise, vibrations which are not related to the characteristics of the thrust stand, and resolution of the displacement sensor, we regard it as over all resolution of the displacement measurement system. Finally a mean square value of the noise is expressed as,

$$E(x_n^{\ 2}) = N_m^{\ 2} \frac{1}{\varsigma} + N_r^{\ 2} \tag{14}$$

In this study, by using the evaluation of Signal and Noise above, SN ratio: R_{SN} is defined as

$$R_{SN} = \frac{x_{\max}}{\sqrt{E(x_n^{\ 2})}} \tag{15}$$

Substituting Eq. (8) and Eq. (14) into Eq. (15) gives

$$R_{SN} = \frac{\exp\left(-\varsigma \dfrac{Cos^{-1}(\varsigma)}{\sqrt{1-\varsigma^2}}\right)}{\sqrt{(N_m / A)^2 \dfrac{1}{\varsigma} + (N_r / A)^2}} \tag{16}$$

expressing that the SN ratio depends on only the damping ratio ζ and two parameters N_m/A and N_r/A. Figure 6 shows the SN ratio dependence on a) N_m/A when N_r/A is a constant and b) N_r/A when N_m/A is a constant. From those graphs, it is shown that SN ratio has the maximum value at a certain damping ratio. It is optimum damping ratio ζ_{out}. In addition, from Eq. (16), it is clear that ζ_{out} depends on only the ratio of N_m to N_r, namely N_m/N_r. Fig. 6 shows the ζ_{out} dependence on N_m/N_r. With reference to Fig. 7, we consider two limit cases of ζ_{out}: N_m/N_r is zero or infinity. At former case, ζ_{out} becomes zero, which means that a damper is not need when there is no external vibration. On the other hand, when a displacement measurement system is ideal, ζ_{out} becomes a constant value: 0.551.

Under the condition of this study, the optimum damping ratio was 0.16. This value was calculated by substituting the measured standard deviation of the balance motion and the resolution of the displacement sensor into Eq. (14). The damping ratio of the thrust stand dealt here was 0.043. Although it is three times of the optimum damping ratio, the SN ratio is roughly equal to the SN ratio at optimum. It arises from the fact that SN ratio is gently varying against a damping ratio as shown in Fig. 6. In fact, the rise is approximately only 25 %.

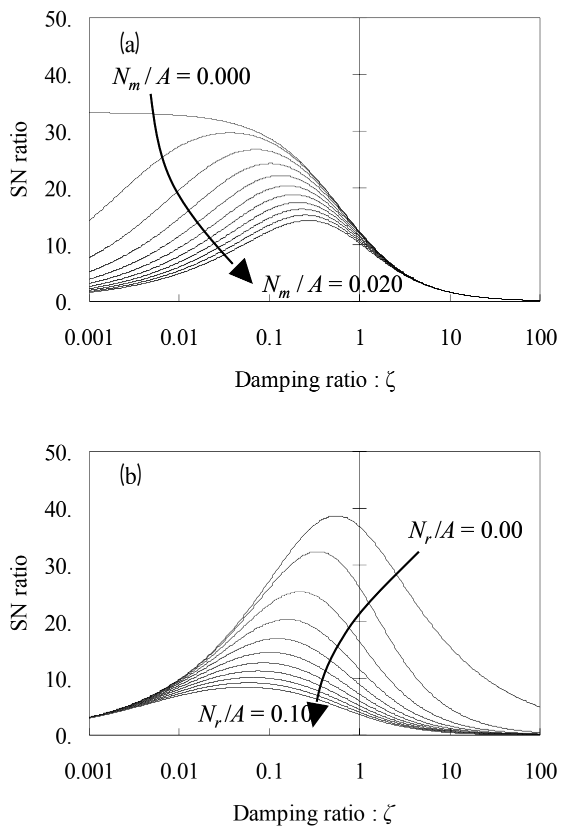

Fig. 6 SN ratio dependence on damping ratio

5.2 Measurement of vibrational noise

We measured dependence of noise on the damping ratio, in order to justify the evaluation of the above mentioned SN ratio. Signal, that is the maximum value of an impulse response, clearly depends on damping ratio according to Eq. (8). Therefore the evaluation of the SN ratio can be verified by measuring only the noise dependence.

Noise was measured by the following sequence. The thrust stand was installed in a vacuum chamber, and the damper was set for certain strength. After measurement of damping ratio, the door of the chamber was closed, and the thrust stand was left during an hour (however the chamber was not evacuated). The vibration of the thrust stand was measured during 1000 s. Its record was

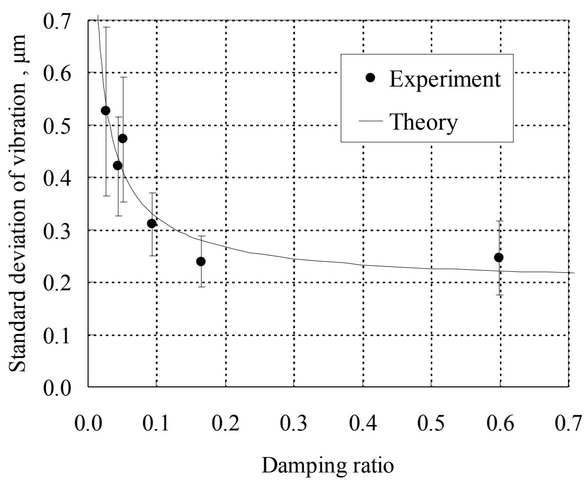

Fig. 7 Induced vibration dependence on damping ratio

separated into slices of 20 s, and the mean square value was calculated for each slice. The averaged value of the mean square value of all slices was defined as noise. That experiment was repeated 6 times with respectively different damping ratio.

Figure 7 shows the noise dependence on damping ratio with the theory of the Eq. (14). The result of the experiment showed good agreement with the theory; however, it should be note that Eq. (14) includes two parameters.

5.3 Influence of parameters

Here, according to Eq. (16), we discuss about other characteristics of a thrust stand. From Eq. (16), SN ratio depends on only two indexes N_m/A and N_r/A. They represent respectively the amount of external vibrations and the resolution of the displacement measurement system; which is more dominative depends on the experimental conditions. They are expanded as

$$N_m / A = \frac{l_G M}{I l_I} \left(\frac{J}{k} \right)^{1/4} \frac{\pi S_0}{2} \quad (17)$$

$$N_r / A = \frac{\sqrt{Jk}}{I l_I l_m} N_r \quad (18)$$

The effects of each parameter on noise are shown in Table 1. The number in parentheses in Table 1 shows the power by which Eq. (17) or Eq. (18) is proportional to each parameter.

A length from the rotational axis to a thruster l_I has an effect linearly on both N_m/A and N_r/A; it is one of the most important parameter. On the other hand, a length from the rotational axis to a measurement sensor l_m has an effect on only N_r/A.

We should position light counter weight far away from the rotational axis lest M increases, total mass of the thrust stand M has a more effect on N_m/A than the momentum inertia J. In principle, we can have center of gravity l_G zero by adjusting a counterweight, and eliminate Eq. (17) completely. However it is impossible because of difficulty to precisely know the position of gravity center. Therefore l_G remains at finite value.

Table 1 The effects of each parameter on noise

	N_m /A	N_r /A
l_I	○ (-1)	○ (-1)
l_m		○ (-1)
M	○ (+1)	
J	△ (+1/4)	△ (+1/2)
l_G	○ (+1)	
k	△ (-1/4)	△ (+1/2)

6. Summary

In this study, a torsional type thrust stand was designed, and it was shown that the thrust stand could measure impulse bits ranging from 10 to 1000 μNs. In addition, it is shown that an optimum damping ratio exists which provides a maximum SN (signal-to-noise) ratio.

References

[1] Kennetb W. Stark, Thomas Dennis, Daniel McHugh, and Thomas Williams, "Design and Development of a Micropound Extended Range Thrust Stand (MERTS)," NASA Technical Note D-7029, August 1971.

[2] Thomas W. Haag, "Thrust Stand for Pulsed Plasma Thruster," Rev. Sci. Instrum., **68**(5), pp.2060-2067, May 1997.

[3] M. J. Wilson, S. S. Bushman, and R. L. Burton, "A Compact Thrust Stand for Pulsed Plasma Thrusters," 25th International Electric Propulsion Conference, Cleveland, Ohio, August 24-28 1997. IEPC 97-122.

[4] A. J. Jamison, A. D. Katsdever, and E. P. Muntz, "Accurate Measurement of Nano-Newton Thrust for Micropropulsion System Characterization," 27th International Electric Propulsion Conference, Pasadena, California, October 15 – 19, 2001. IEPC-01-236

[5] J. K. Ziemer, "Performance Measurement Using a Sub-Micronewton Resolution Thrust Stand," 27th International Electric Propulsion Conference, Pasadena, California, October 15 – 19, 2001. IEPC-01-238.

[6] R. Yanagi and I. Kimura, "New Type of Target for the Measurement of Impulse Bits of Pulsed Plasma Thrusters," J. Spacecr. Rockets, **19**, NO.3, pp.246-249, 1982.

[7] M. Igarashi, N. Kumagai, K. Sato, K. Tamura, and H. Takegahara, "Performance Improvement of Pulsed Plasma Thruster for Micro Satellite," International Electric Propulsion Conference, Pasadena, California, Oct. 15-19 2001. IEPC 01-152.

[8] A. Kakami, H. Koizumi, K. Komurasaki, and Y. Arakawa, "Liquid Propellant PPT Performance," 23rd International Symposium on Space Technology and Science, Matsue, May 26 – June 2, 2002. ISTS 2002 b-15.

[9] D. E. Newland, "An introduction to random vibrations and spectral analysis," 2nd ed., Longman Scientific & Technical, New York, 1984.